ELSEVIER

Journal of Fluids and Structures 19 (2004) 1049–1059

JOURNAL OF FLUIDS AND STRUCTURES

www.elsevier.nl/locate/jnlabr/yjfls

Flow past a circular cylinder over a free surface: Interaction between the near wake and the free surface deformation

S.J. Lee*, Daichin[1]

Department of Mechanical Engineering, Pohang University of Science and Technology, San 31, Hyoja-Dong, Nam gu, Pohang 790-784, Korea

Received 15 August 2003; accepted 26 July 2004
Available online 5 October 2004

Abstract

Air-flow around a circular cylinder placed above a free surface and liquid flow under the free surface were investigated experimentally in a wind/wave tunnel. The cylinder spanned the tunnel test-section and was oriented normal to the freestream direction. The main objective of this study was to investigate the interaction of the cylinder wake with the free surface. The flow structure was analyzed for various gap widths, H, between the cylinder and the free surface using a digital particle image velocimetry (PIV) system with a spatial resolution of 2048×2048 pixels. The Reynolds number based on the cylinder diameter was 3.3×10^3. For each experimental condition, 400 instantaneous velocity fields were measured and ensemble-averaged to obtain spatial distributions of the mean velocity and turbulence statistics. The results showed that the cylinder near-wake inclined upward due to the influence of the free surface elevation. Vortices were shed, even at a small gap ratio of $H/D = 0.25$, where D is the cylinder diameter. Strong jet-like flow appeared in the gap beneath the cylinder. At a gap ratio of $H/D = 0.50$, the jet flow exhibited a quasi-periodic vibration with a period of 2–3 s. The free surface deformation was caused by the pressure difference in the air-flow immediately above it. As the gap ratio increased, the inclination angle of the wake and the height of the free surface elevation decreased gradually. The liquid flow under the free surface followed a convective flow motion, and the range of the convection depended on the gap width between the cylinder and the free surface.

1. Introduction

Periodic vortex shedding and coherent structures in the wake behind a bluff body are related to many aerodynamic problems, such as aerodynamic drag, flow-induced vibration, and aero-acoustic noise. In the past two decades, the flow around a bluff body located adjacent to a solid boundary has received considerable attention. The formation of vortices behind a bluff body and the vortex shedding frequency are strongly influenced by the nearby boundary layer, compared to flows that have a body-wake in an unbounded medium.

Several previous studies have focused on the flow structure of a circular cylinder near a solid plate or the wake disturbance due to the presence of a solid boundary. Bearman and Zdravkovich (1978) investigated the flow characteristics around a circular cylinder near a flat plate for various gap widths. A cylinder of diameter D was

*Corresponding author. Tel.: +82-54-279-2169; fax: +82-54-279-3199.
E-mail address: sjlee@postech.ac.kr (S.J. Lee).
[1]Present address: Institute of Applied Mathematics and Mechanics, Shanghai University, 200072, China.

0889-9746/$ - see front matter © 2004 Elsevier Ltd. All rights reserved.
doi:10.1016/j.jfluidstructs.2004.06.006

embedded in a boundary layer that had a thickness of $0.8D$. Regular vortex shedding was suppressed for small gap ratios less than the critical gap ratio of 0.3, and the Strouhal number St remained almost unchanged for gap ratios greater than the critical value. Angrilli et al. (1982) investigated wall effects on the vortex shedding frequency at low sub-critical Reynolds numbers for which the boundary layer thickness was equal to $0.25D$. In this case, the vortex shedding frequency increased as the cylinder approached the wall. Taniguchi and Miyakoshi (1990) measured the fluctuating fluid forces and pressure distributions acting on a cylinder located near a plane wall to study the effect of the boundary layer thickness on the critical gap ratio. Their critical gap ratio increased with the boundary layer thickness. However, the Strouhal number, St, remained equal to approximately 0.2 and was nearly independent of the boundary layer thickness. Lei et al. (1999) found that the aerodynamic forces acting on a cylinder were more dependent on the gap ratio than on the boundary layer thickness. Their critical gap ratio decreased slightly as the boundary layer thickness increased, contrary to the results of Taniguchi and Miyakoshi (1990). In addition, St did not change significantly with either the gap ratio or the boundary layer thickness. Choi and Lee (2000) investigated the ground effect of flow around an elliptic cylinder embedded in a turbulent boundary layer.

However, the flow around a bluff body located above a free surface has received little attention. The flow interaction between the body-wake and the free surface deformation are closely related to several engineering problems, such as the wing ground effect and that of wind over marine structures on ocean platforms above sea level. This study investigated the flow field around a circular cylinder mounted horizontally over a free surface and the effects of the free surface elevation on the formation of the cylinder near-wake. Modification of the flow field under the free surface due to the presence of the cylinder was also analyzed.

2. Experimental apparatus and conditions

The experiment was performed in a small-scale wind/wave tunnel with a test-section of $1850 \times 150 \times 350$ mm ($L \times W \times H$). The water depth in the test-section was 200 mm. Fig. 1 shows the tunnel test-section and experimental setup. To avoid surface wave reflections from the solid wall downstream, a wave absorber was placed at the end of the water tank. A circular cylinder with a diameter of $D = 8$ mm was installed parallel to the water surface and normal to the freestream direction. The vertical distance from the free surface to the bottom of the cylinder was denoted by the gap width, H, as shown in Fig. 2. The nondimensional gap ratio $h^* = H/D$ was used to represent the results. The approaching freestream velocity was fixed at $U_0 = 6.12$ m/s, for which the corresponding Reynolds number ($U_0 D/\nu$) based on the cylinder diameter was 3.3×10^3. The turbulence intensity of the freestream flow was less than 0.1%.

The instantaneous velocity fields in the water and air in the wind/wave tunnel were measured separately using a two-frame PIV system. The PIV system consisted of a high-resolution CCD camera, a dual-head Nd:YAG laser, a synchronizer, and optics. The CCD camera (Kodak ES4.0) had a spatial resolution of 2048×2048 pixels with a maximum frame rate of 15 frames per second (fps). The Nd:YAG laser provided a maximum output energy of 25 mJ per pulse. The Nd:YAG laser and the CCD camera were synchronized using a delay generator. The central cross-section of the flow field was illuminated from both sides at the top and bottom of the wind/wave tunnel. Atomized olive oil particles with an average diameter of 2–3 μm were used as seeding particles in the air, and Vestosint® 1118 particles with a mean diameter of 37 μm were used as tracer particles in the water.

The experiment was performed using five different gap ratios: $h^* = 0.25$, 0.50, 0.75, 1.00, and 1.25. For each gap ratio, about 400 particle image pairs were captured to obtain instantaneous velocity fields that were ensemble-averaged to calculate the spatial distributions of the turbulent statistics such as mean velocity, vorticity, and turbulence intensity.

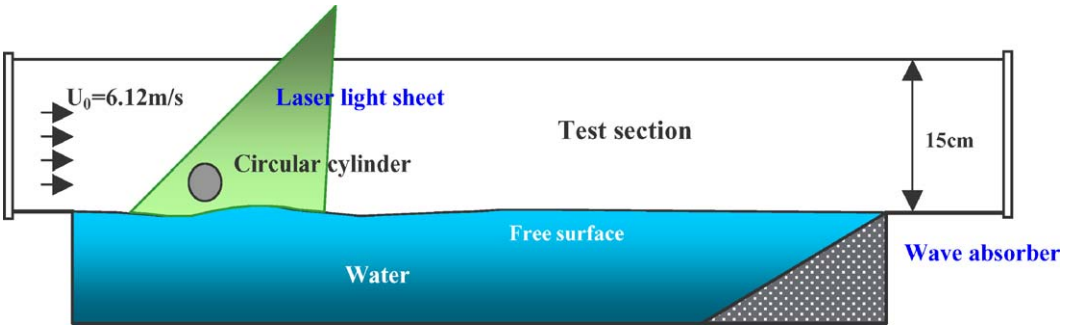

Fig. 1. Schematic diagram of wind-wave tunnel and experimental setup.

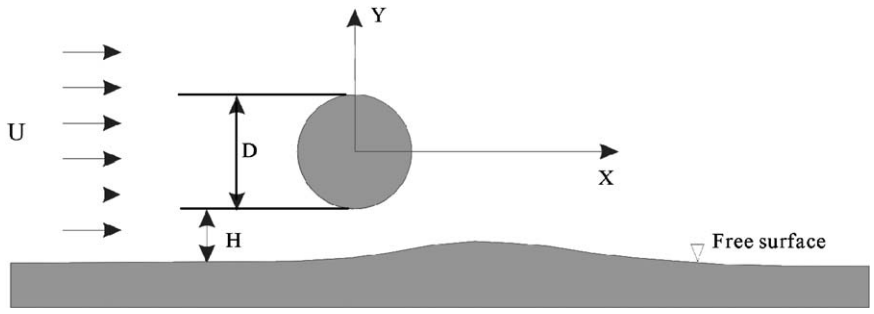

Fig. 2. Definition of flow and geometrical parameters.

Since the cylinder was installed very close to the entrance of the test-section, the boundary layer over the water surface had not completely developed at the cylinder location. Even at a gap ratio of $h^* = 0.25$, the cylinder was located outside the boundary layer. Therefore, in this study, the boundary layer was thinner than the gap width between the cylinder and the free surface. At the cylinder location, the thickness of the boundary layer above the free surface was about $0.2D$. Due to this arrangement, we focused more on the effect that the free surface elevation had on the flow structure of the wake behind the cylinder than on the flow interaction between the boundary layer and the wake behind the cylinder.

3. Results and discussion

3.1. Instantaneous velocity field

Fig. 3(a) shows the instantaneous velocity field at a gap ratio of $h^* = 0.25$. From this result, we can see that the free surface had a significant influence on the flow field. When the gap ratio was small, the cylinder blocked the airflow passing through the gap above the free surface, decreasing the flow speed remarkably and forming a vortex in front of the cylinder. The rapid reduction of the flow velocity increased the pressure of the airflow, depressing the level of the free surface immediately in front of the cylinder. After passing through the gap between the cylinder and the free surface, the airflow speed increased and a jet-like flow formed. The airflow speed was much greater than that at the lower front corner of the cylinder. The resultant low pressure caused the free surface beneath the jet-like flow to elevate gradually.

The flow viscosity also contributed to the free surface distortion, but its effect seemed to be much smaller than the air pressure variation. The shape of the free surface did not change noticeably with time, i.e., the deformed free surface maintained its shape. In addition, because the flow velocity under the cylinder was less than that above its upper surface, the cylinder was subjected to an upward lift force. Due to inclination of the free surface and the jet-like flow, the cylinder wake inclined slightly upward and the vortices shed from the cylinder moved in the same direction. The distance between the two shear layers behind the cylinder was less than that of a cylinder in an unbounded flow field.

At a gap ratio of $h^* = 0.50$, the flow field exhibited a quasi-periodic vibration, as shown in Fig. 3(b). At time t, the basic flow pattern was similar to that for $h^* = 0.25$: vortices were shed from the cylinder, and the jet-like flow in the gap was attached to the free surface. At time $t + \Delta t$, however, the slope of the inclined surface increased and the airflow beneath the cylinder completely detached from the free surface and formed a jet-like flow. In addition, a large-scale clockwise-rotating vortex existed in the region between the jet and the free surface. The lower shear layer of the cylinder wake inclined upward and vortices were formed farther away from the cylinder base, compared with what was observed at time t. The jet-like flow showed a quasi-periodical variation in the region between the free surface and cylinder wake. When we checked the 400 instantaneous velocity fields obtained consecutively at a rate of 4 fps, this phenomenon repeated every 8–10 velocity fields, which gave a corresponding period of approximately 2–3 s. Reflecting the vibration of the jet-like flow, the steepness of free surface behind the crest changed periodically. As the jet-like flow moved away from the free surface, the steepness of the back slope increased due to the increase in the air pressure above the free surface. Conversely, the back slope decreased when the jet attached to the free surface. Nevertheless, throughout the variation period, the front slope of the free surface did not change significantly. All of these results indicate that the free surface deformation was primarily caused by the difference in the air pressure distribution above the surface. In addition, the velocity field under the cylinder also changed, altering the lift force acting on the cylinder.

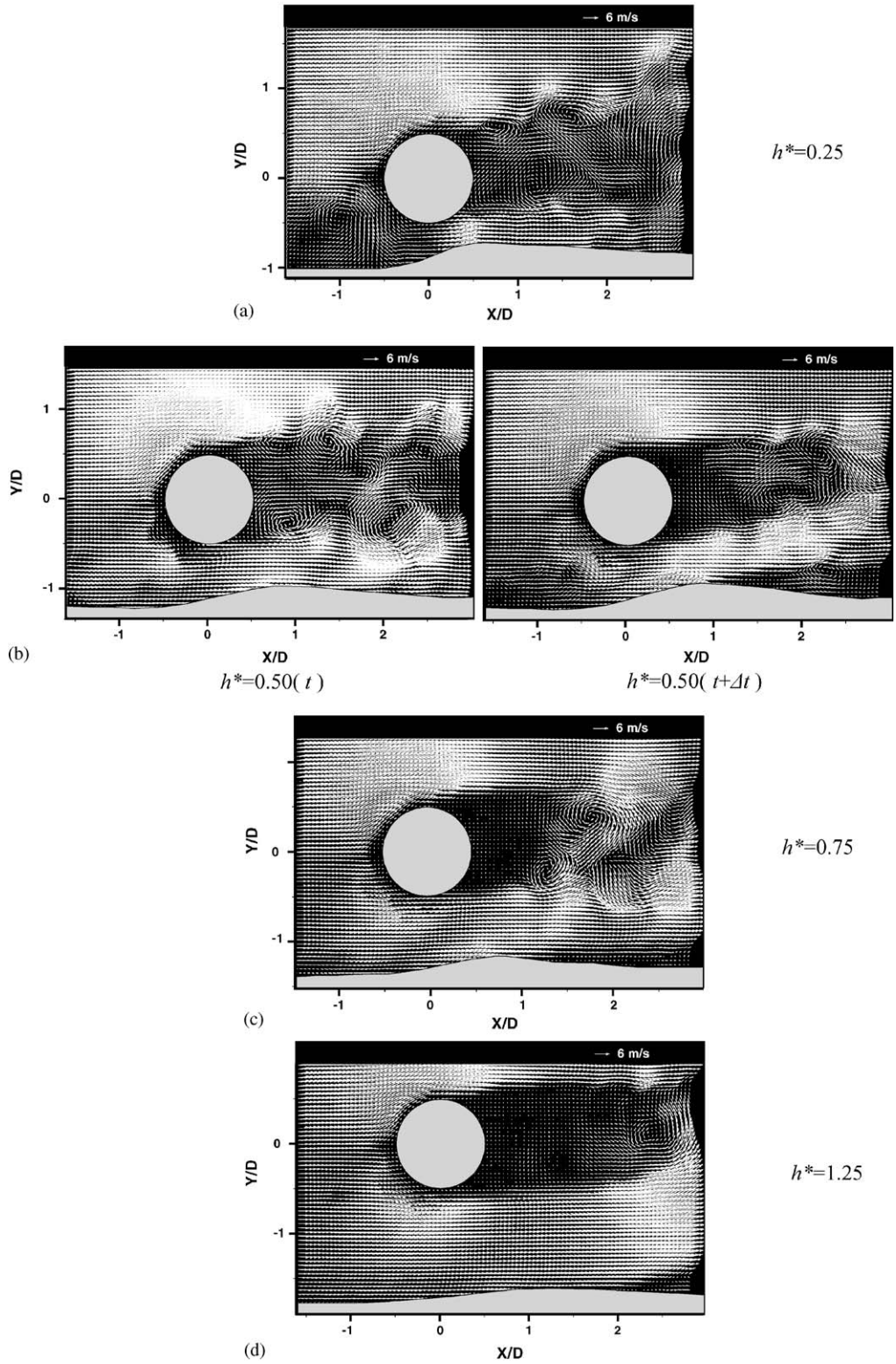

Fig. 3. Instantaneous velocity fields around a circular cylinder over the free surface.

Sheridan et al. (1995, 1997) observed similar flow patterns for a circular cylinder submerged under a free surface. They found two different metastable flow patterns in the region between the cylinder and the free surface, which depended on the flow parameters and the depth of cylinder submergence. Similarly, in our study, when the jet flow detached from the free surface completely, a large-scale vortex formed between the jet and the free surface. However, the free surface distortion differed in the two cases. For the circular cylinder submerged under the free surface, the surface distortion was accompanied by localized wave breaking, with a strong vertical velocity component. In contrast, in this study, the free surface seemed to be distorted by a self-adjusting pressure distribution over the free surface. Therefore, the profile of the free surface distortion was rather smooth and mild.

When the gap ratio was increased to $h^* = 0.75$, the blockage effect of the gap was reduced. Since the air pressure difference between upstream and downstream from the gap decreased, the free surface elevation was reduced and the wave slope decreased compared to that observed with $h^* = 0.25$. In the downstream region behind the crest, a laminar boundary layer formed above the free surface. However, the pressure variation in the boundary layer was too small to affect the free surface elevation. In addition, due to the increased gap ratio, the upward push of the jet-like flow from the lower shoulder of the cylinder was also weakened and the upward inclining angle of the lower shear layer was reduced. Since the shear layer from the upper side of the cylinder was nearly horizontal, the wake width behind the cylinder was slightly wider than that observed for smaller gap ratios. Since this delayed the flow interaction between the upper and lower shear layers, the first vortex was shed approximately $1D$ downstream from the cylinder.

As the gap ratio increased from $h^* = 0.75$ to 1.00, the general flow patterns did not change, except for a further decrease of the upward inclining angle of the cylinder wake. At the largest gap ratio tested in this study, $h^* = 1.25$, the free surface deformation was weak and the free surface elevation had a long wavelength. The vortex formation region in the cylinder wake was extended, compared to that observed for smaller gap ratios, and regular vortex shedding occurred farther downstream. Moreover, the lower shear layer no longer declined upward, but remained nearly horizontal. This implies that the effect of the free surface deformation on the cylinder wake was reduced greatly. When the gap ratio exceeded $h^* = 0.75$, both the upper and lower sides of the cylinder had similar flow speeds, so that the lift force acting on the cylinder approached a state of balance.

For a fully submerged circular cylinder, regular vortices are shed by the symmetric interaction of the two shear layers formed on both sides of the cylinder (Gerrard, 1966). Bearman and Zdravkovich (1978) showed that vortex shedding from a cylinder located near a solid flat plate was suppressed when h^* was less than about 0.3. The suppression of regular vortex shedding was closely linked with the asymmetric development of the vortices behind the cylinder. The vortex on the freestream side grew larger and stronger than the vortex near the solid wall.

In this study, regular vortex shedding still occurred at a gap ratio $h^* = 0.25$. One reason for this phenomenon may be the fact that the bottom gap was wider than the boundary layer thickness over the free surface. Therefore, the lower shear layer of the cylinder wake did not merge into the free surface boundary layer. For small gap ratios ($h^* = 0.25$ and 0.50), the vortices shed from the lower side of the cylinder seemed to be of reasonable strength. Decreasing the gap ratio beyond $h^* = 0.25$ caused the free surface to attach to the bottom of the cylinder, thereby blocking the airflow beneath the cylinder.

As the gap ratio decreased, the size of the vortex formation region behind the cylinder also decreased. In addition, the speed of the jet-like flow under the cylinder increased and even exceeded the freestream velocity. The entrainment of freestream flow in the lower shear layer started to occur farther downstream from the cylinder. Consequently, some of the high-speed gap flow was entrained into the wake region at a location closer to the cylinder base, shrinking the formation region. Another factor that contributed to the shrinking of the formation region for small gap ratios was the steep angle of the front slope of the free surface elevation beneath the cylinder. This caused the lower shear layer to bend upwards, increasing the vortex shedding frequency and reducing the width of the formation region.

For a cylinder located above a solid flat plate, the maximum gap flow speed occurs at the narrowest gap width, located just beneath the cylinder. In this study, however, the maximum free surface elevation was located downstream of the cylinder instead of directly underneath, and the maximum gap flow speed occurred in the middle of the gap between the cylinder and the upwards slope of the free surface.

3.2. Mean velocity field

For each gap ratio, 400 instantaneous velocity fields were measured and ensemble-averaged to obtain spatial distributions of the mean flow structure. Fig. 4 shows contour plots of the streamlines for four different gap ratios. The two large-scale eddies that formed behind the cylinder clearly had different structures, depending on the gap ratio. At a small gap ratio of $h^* = 0.25$, the lower eddy dominated the flow field in the near wake region. Its vortex strength and size were much larger than those of the upper eddy, causing the upper vortex to eventually diffuse. As the gap ratio increased, the strength and size of the upper vortex were enhanced gradually. At a gap ratio of $h^* = 1.25$, the two eddies

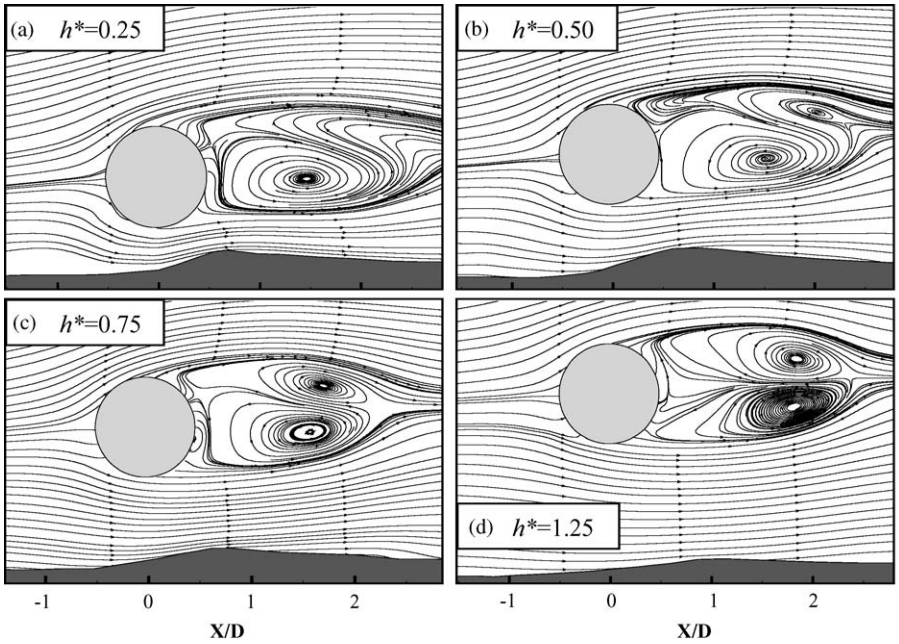

Fig. 4. Contour plots of streamlines for four different gap ratios.

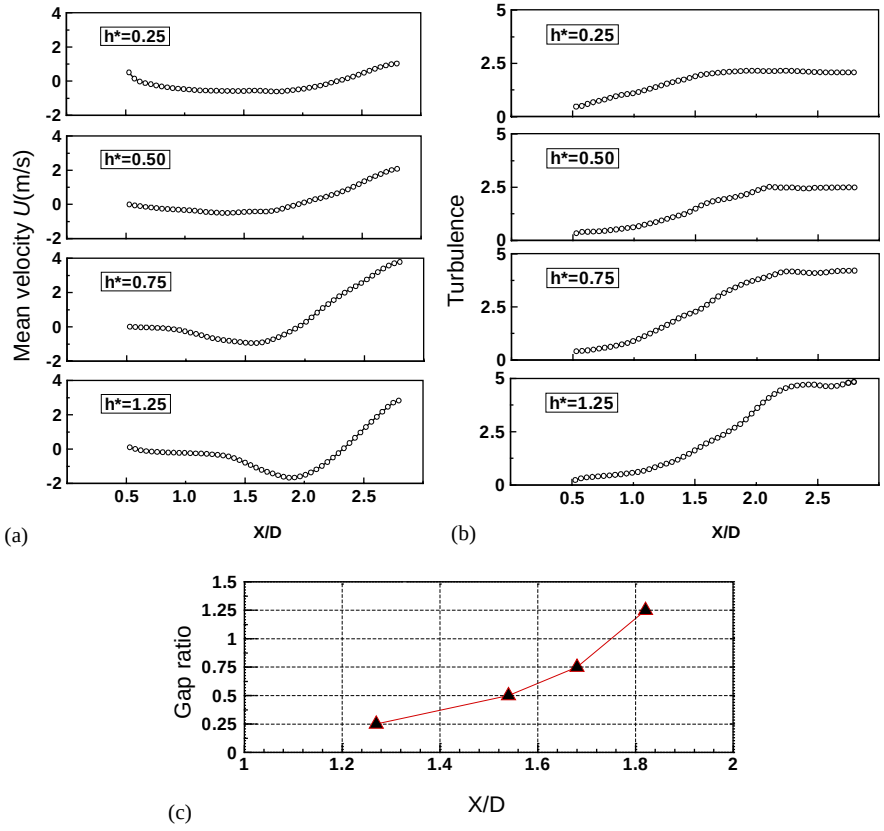

Fig. 5. Profiles of (a) streamwise mean velocity (b) streamwise turbulence intensity $\sqrt{\overline{u'^2}}/U$ along cylinder wake center-line and (c) length of vortex formation region.

were similar in size and nearly symmetric with respect to the wake center-line. However, the lower vortex was still slightly stronger than the upper one. As the gap ratio increased, the downstream distance between the two eddies and the cylinder base also increased, i.e., the size of the formation region was elongated, as expected from the instantaneous velocity field results discussed previously.

The streamwise mean velocity and turbulence intensity distributions along the wake center-line were extracted from the ensemble-averaged velocity fields. The results are shown in Fig. 5. The streamwise mean velocity decreased gradually with the distance downstream along the wake center-line, and then started to increase near the end of the vortex formation region. Behind the formation region, the streamwise mean velocity increased with the gap ratio. For small gap ratios ($h^* = 0.25$ and 0.50), the rate of increase in the mean velocity was mild. For large gap ratios ($h^* = 0.75$ and 1.25), however, the streamwise mean velocity increased rapidly with the distance downstream. Fig. 5(b) gives the streamwise turbulence intensity profiles along the wake center-line. As the gap ratio increased, the streamwise turbulence intensity also increased and the peak location moved away from the cylinder.

Bloor (1963) defined the end of the vortex formation region as the location after which oscillating wake characteristics were observed. This implies that the vortices shed from the two sides of the cylinder cross the wake center axis at the end of the formation region. Since two vortices influence the formation region, one from the upper side of the cylinder and the other from the lower side, the end of the vortex formation region can be estimated by finding the peak location of the streamwise turbulence intensity along the wake center-line. Therefore, in this study, we used a fifth order polynomial curve-fitting technique to find the peak location for each gap ratio. Fig. 5(c) shows the variation in the vortex formation region with the gap ratio. The length of the vortex formation region increased from $x/D = 1.27$ to 1.82 as the gap ratio increased from $h^* = 0.25$ to 1.25. As the gap ratio increased, the length of the vortex formation region initially increased rapidly, and then approached an asymptotic value that corresponded to a cylinder placed in a uniform flow.

3.3. Mean vorticity fields

Fig. 6 illustrates spatial distributions of the spanwise vorticity, ω_z, for four different gap ratios. Irrespective of the gap ratio, the strength and distribution pattern of the negative vorticity in the upper shear layer did not change significantly. On the contrary, the positive vorticity in the lower shear layer of the cylinder wake gradually diffused and its location shifted downstream. At a gap ratio of $h^* = 0.25$, the positive vorticity had large values concentrated in a relatively small region close to the bottom of the cylinder. When the gap ratio increased to $h^* = 1.25$, the region of large positive vorticity elongated greatly in the streamwise direction, and the spatial distribution of the positive and negative vorticity was nearly symmetric with respect to the wake center-line. For $h^* = 0.25$, the airflow around the wave crest of the free surface had negative vorticity. For larger gap ratios, the region of negative vorticity above the free surface moved downstream.

For $h^* = 0.25$, the locus of the positive spanwise vorticity illustrated the upward inclination of the lower shear layer in the cylinder near wake. The inclination angle was approximately parallel to the upward slope of the free surface. A similar trend occurred for larger gap ratios, indicating that the formation of the lower shear layer was closely related to the front slope of the free surface. For larger gap ratios, the steepness of the surface elevation decreased as did the upward inclining angle of the cylinder wake.

3.4. Turbulence intensity

Streamwise turbulence intensity distributions are shown in Fig. 7. Irrespective of the gap ratio, the general distribution of the streamwise turbulence intensity in the cylinder wake looked similar, with large values in the upper and lower shear layers at the end of the formation region. However, the turbulence intensity varied remarkably in the gap region according to the gap ratio. At a small gap ratio of $h^* = 0.25$, the turbulence intensity had large values in the gap just beneath the cylinder, as shown in Fig. 7(a). Since the flow choked in the gap, the flow was accelerated along the upward slope of the free surface to form a jet-like flow. Therefore, the maximum turbulence intensity was located in this region. Although the jet-like flow did not separate from the free surface in the downstream region, there was still relatively high turbulence intensity in the boundary layer above the free surface. The jet-like flow separated from the free surface at a gap ratio of $h^* = 0.50$. Here, the maximum turbulence intensity occurred in the boundary layer over the free surface, where it was even greater than that in the shear layer behind the cylinder. As the gap ratio increased, the turbulence intensity in the region above the free surface decreased gradually and the wake region of high turbulence intensity shifted downstream.

Comparing the spatial distributions of the streamwise turbulence intensity, spanwise vorticity, and streamlines for each gap ratio, we found that the turbulence intensity had large values in the region where the freestream was entrained

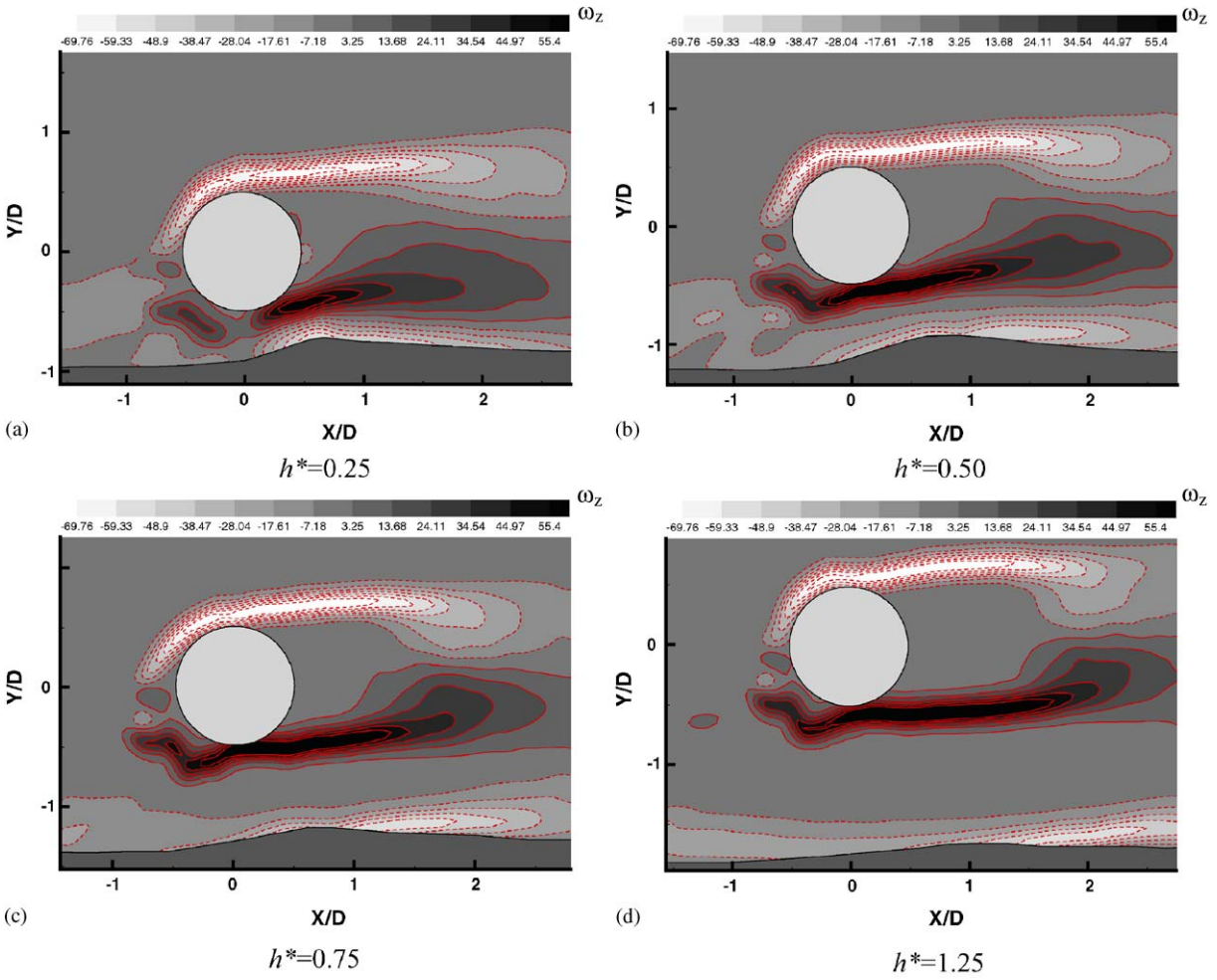

Fig. 6. Contour plots of spanwise vorticity ω_z.

into the wake region and where the vorticity started to be diffused. As the gap ratio increased, the region of very small turbulence intensity just behind the cylinder expanded. It is also interesting to note that the lower shear layer of the cylinder wake had a greater turbulence intensity compared to the upper shear layer due to active interactions with the gap flow.

3.5. Free surface elevation

To investigate the free surface elevation and effect of air-flow on the liquid flow beneath the free surface, we measured the velocity fields under the free surface for different gap ratios. The liquid flow just beneath the air/water interface was driven by the air-flow due to the viscous drag effect. If we neglect interface slip and interfacial entropy, the liquid velocity can be assumed to equal the air velocity at the interface. As mentioned before, the free surface was deformed primarily due to the air-pressure distribution over the surface.

Fig. 8 shows typical instantaneous velocity fields and the corresponding streamlines of water flow under the free surface. At small gap ratios of $h^* = 0.25$ and 0.50, the liquid flow near the interface had a velocity less than 5 cm/s; this decreased with increasing water depth. In the region upstream from the wave crest, especially beneath the cylinder, the streamlines paralleled the free surface profile.

The flow velocity in the upstream region exceeded that in the downstream region. At a gap ratio of $h^* = 0.50$, a large-scale eddy formed under the wave crest. When the gap ratio increased to $h^* = 0.75$, the eddy beneath the crest was enhanced and the flow velocity under the free surface increased compared to that observed for smaller gap ratios. Some

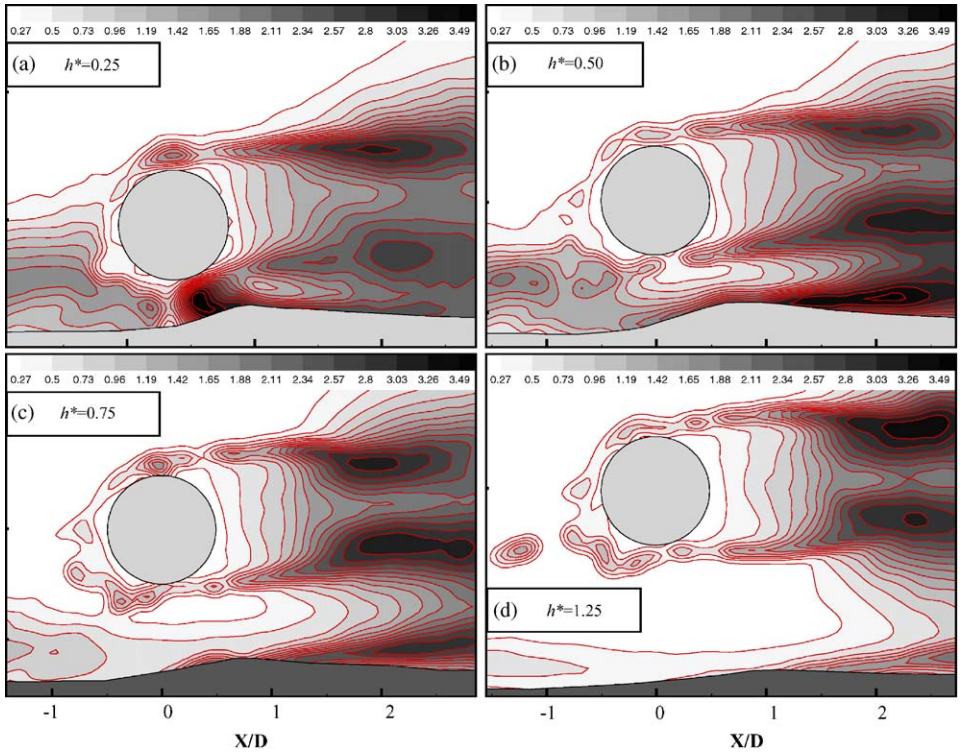

Fig. 7. Variation of streamwise turbulence intensity distribution.

of the shear flow behind the crest was entrained into the large-scale eddy, while the rest moved downstream. Compared to the case with $h^* = 0.50$, the center of the eddy moved toward the wave crest, while the front and back slopes of the free surface elevation were similar. When $h^* = 1.25$, the free surface elevation became milder, although the large-scale eddy still existed beneath the crest; however, the eddy was deformed and its strength was markedly reduced.

In order to replenish the region of flow driven downstream by the air-flow, the fluid in the bottom region was entrained toward the free surface. This resulted in a large-scale convective flow motion, which eventually formed a large swirling flow under the wave crest of the free surface. At $h^* = 0.25$, convective flow motion appeared throughout the entire liquid body. For $h^* = 1.25$, however, the region of convective motion was largely reduced compared to that observed for smaller gap ratios.

4. Conclusions

The flow characteristics of the near wake behind a circular cylinder located above a free surface and the liquid flow under the free surface were investigated experimentally for different gap widths between the cylinder and the free surface.

Vortices were shed regularly, even at a gap ratio of 0.25. The lower shear layer of the cylinder wake was inclined upward, enhancing the flow interaction with the upper shear layer. The upward movement of the lower shear layer reduced the wake width. As the gap ratio increased, the distance between the two shear layers that separated from the cylinder also increased, and the vortex formation region was elongated. However, the vorticity distribution in the cylinder wake did not show any notable variation with respect to the gap ratio.

The free surface elevation was mainly caused by the air pressure distribution just above the free surface. With an increase in the gap ratio, the surface elevation decreased and the front slope ahead of the wave crest became less steep. Convective flow motion dominated in the region beneath the wave crest of the free surface; the range of the convection depended on the gap width between the cylinder and the free surface. In addition, the deflection of the lower shear layer of the cylinder wake was closely related to the upward slope of the free surface in front of the wave crest.

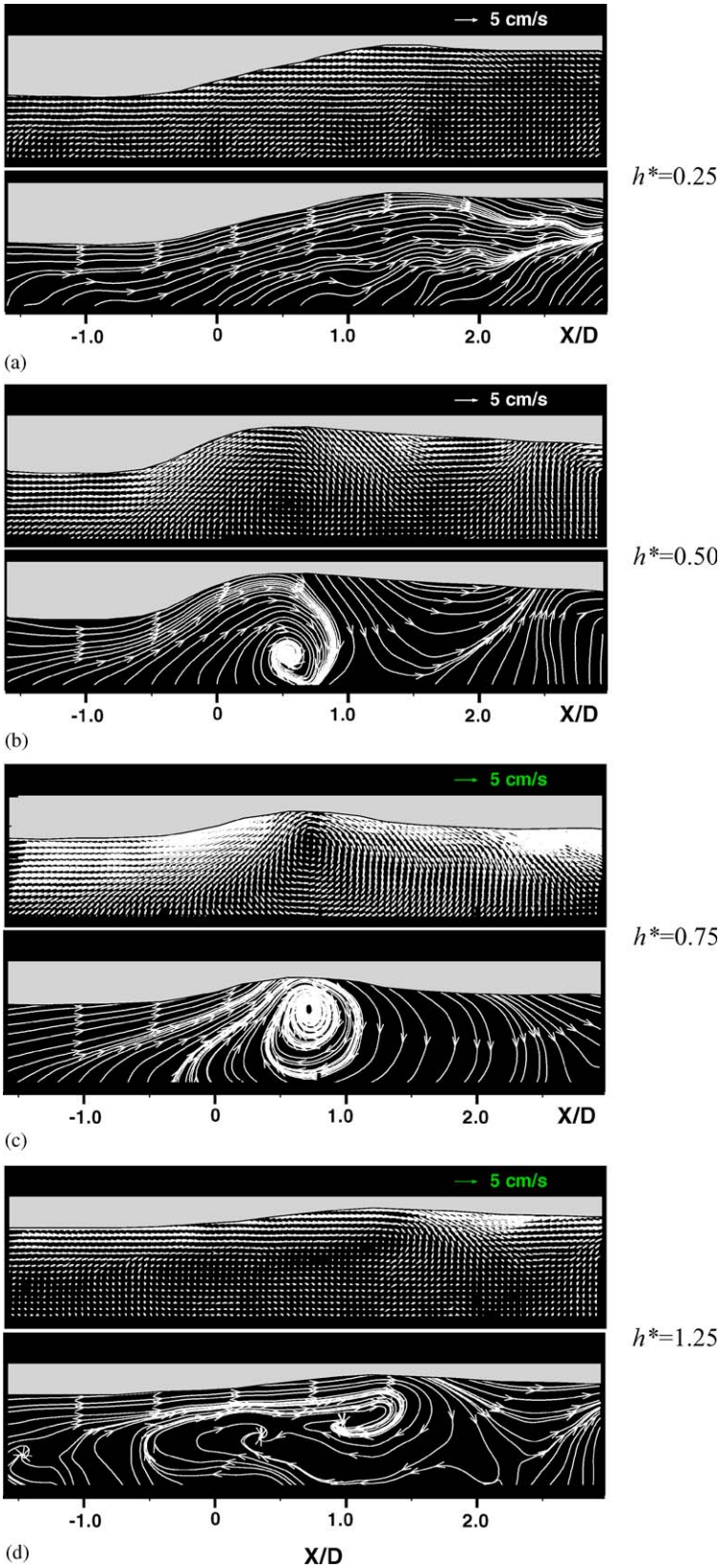

Fig. 8. Instantaneous velocity fields and streamlines of water flow under the free surface.

Acknowledgement

This work was supported by the National Research Laboratory (NRL) program of the Ministry of Science and Technology, Korea.

References

Angrilli, F., Bergamaschi, S., Cossalter, V., 1982. Investigation of wall-induced modifications to vortex shedding from a circular cylinder. ASME Journal of Fluids Engineering 104, 518–522.

Bearman, P.W., Zdravkovich, M.M., 1978. Flow around a circular cylinder near a plane boundary. Journal of Fluid Mechanics 89, 33–47.

Bloor, M.S., 1963. The transition to turbulence in the wake of a circular cylinder. Journal of Fluid Mechanics 19, 290–304.

Choi, J.H., Lee, S.J., 2000. Ground effect of flow around an elliptic cylinder in a turbulent boundary layer. Journal of Fluids and Structures 14, 697–709.

Gerrard, J.H., 1966. The mechanics of the formation region of vortices behind bluff bodies. Journal of Fluid Mechanics 25, 401–413.

Lei, C., Cheng, L., Kavanagh, K., 1999. Re-examination of the effect of a plane boundary on force and vortex shedding of a circular cylinder. Journal of Wind Engineering and Industrial Aerodynamics 80, 263–286.

Sheridan, J., Lin, J.C., Rockwell, D., 1995. Metastable states of a cylinder wake adjacent to a free surface. Physics of Fluids 7, 2099–2101.

Sheridan, J., Lin, J.C., Rockwell, D., 1997. Flow past a cylinder close to a free surface. Journal of Fluid Mechanics 330, 1–30.

Taniguchi, S., Miyakoshi, K., 1990. Fluctuating fluid forces acting on a circular cylinder and interference with a plane wall. Experiments in Fluids 9, 197–204.